^{87}Rb NMR of the structural phase transition in RbSCN

R. Blinc, J. Seliger, T. Apih, and J. Dolinšek

J. Stefan Institute, University of Ljubljana, Ljubljana, Slovenia

A. Fuith, W. Schranz, and H. Warhanek

Institut für Experimentalphysik, Universität Wien A-1090, Wien, Austria

(Received 24 October 1994)

The second-order shifts of the ^{87}Rb $1/2 \rightarrow -1/2$ NMR transitions have been measured in RbSCN above and below $T_c = 435$ K for crystal rotations around the a, b, and c axes. Whereas below T_c the ^{87}Rb electric-field gradient (EFG) and chemical shift tensors are compatible with the Rb site symmetry as given by the orthorhombic space group $D_{2h}^{11}(Pbcm)$, this is not the case for the EFG data above T_c. The results show that the symmetry of the high-temperature tetragonal phase is dynamically broken on the Larmor frequency (10^{-8} s) time scale whereas symmetry-breaking terms are averaged out on the "site" splitting, domain splitting, and chemical shift tensor ($\simeq 10^{-2} - 10^{-3}$ s) time scales. ^{87}Rb NMR thus allows for an observation of the phase transition in RbSCN in the "slow motion" regime where the high-temperature phase is seen to consist of a large number of orthorhombic microdomains with lifetimes longer than 10^{-7} s and shorter than 10^{-3} s.

I. INTRODUCTION

Rubidium thiocyanate (RbSCN) undergoes[1] at $T_c = 435$ K a first-order antiferroelectric phase transition from a high-temperature paraelectric tetragonal phase (I) with space group D_{4h}^{18} and two formula units per unit cell ($z = 2$) to a low-temperature antiferroelectric orthorhombic phase (II) with the space group D_{2h}^{11} and four formula units per unit cell ($z = 4$).[2] The transition is generally assumed[3,4] to be connected with a head-tail ordering of the linear SCN$^-$ dipoles which should be dynamically disordered between two equilibrium orientations for $T > T_c$. In the low-temperature phase which is isomorphous[1,4] with KSCN and the orthorhombic phase of NH$_4$SCN,[4] the SCN$^-$ dipoles are ordered in an antiparallel arrangement forming layers perpendicular to the c axis.

Due to the symmetry reduction $D_{4h}^{18} \rightarrow D_{2h}^{11}$ the crystal splits below T_c into four domains:[5] two 90° rotational domains and two antiphase domains. The shift of the Rb$^+$ or K$^+$ ions from their position on the fourfold rotation axis is linearly coupled[6] to the orientational degree of freedom of the SCN$^-$ ions. The Rb ions should be thus shifted from their high-temperature position along the $+a$, $-a$, $+b$, and $-b$ directions in the four different domains of phase II (Fig. 1).

Diffuse neutron-scattering measurements[7] have shown that the tetragonal high-temperature phase of RbSCN can be roughly described as a superposition of the four types of microdomains of Fig. 1. The superposition is static on the neutron-scattering times scale.[7] The size of the microdomains is between 50–100 Å. Disordering occurs by increased formation of antiphase domain boundaries whereas within the bulk of the domains the SCN$^-$ groups remain locally in an ordered configuration even close to the melting point.

To see whether we indeed deal above T_c with a static superposition of microdomains or a dynamic disorder in-

volving relatively slow head-tail flipping of the SCN$^-$ groups we decided to perform a ^{87}Rb ($I = 3/2$) NMR study of RbSCN. We also wanted to throw some additional light on the coupling between the SCN$^-$ and Rb$^+$ ion motion and the time scale of the structural fluctuations.

II. EXPERIMENT

Fourier transform ^{87}Rb $1/2 \rightarrow -1/2$ quadrupole perturbed NMR spectra were recorded at a Larmor frequency $\omega_L / 2\pi = 88.39$ MHz in a superconducting magnet
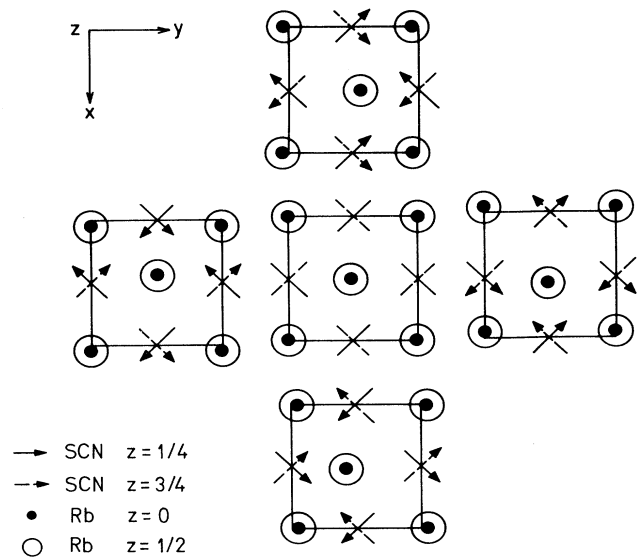

FIG. 1. Four domain states appearing in the orthorhombic phase of RbSCN. The tetragonal phase is shown for comparison.

with $B_0 = 6.34$ T. The spectra were obtained with the solid echo $(\pi/2)_x - (\pi/2)_y$ pulse sequence.

The monodomain single crystal grown at room temperature (i.e., at $T < T_c$) was rotated around three mutually perpendicular crystallographic axes a, b, and c to determine the electric-field gradient (EFG) tensors at the Rb sites. After heating above T_c and subsequent cooling below T_c, domains were formed which could be observed by [87]Rb NMR.

III. STRUCTURAL CONSIDERATIONS

According to the crystal structure,[1,4] there are two [87]Rb nuclei in the primitive cell above T_c. Both are physically and chemically equivalent and lie on the fourfold rotation axis. The two [87]Rb EFG tensors should therefore be axially symmetric $V_{XX} = V_{YY}$ and the largest principal axis V_{ZZ} should point along the fourfold axis. Below T_c there should be four chemically equivalent nonaxially symmetric [87]Rb EFG tensors in the unit cell. They form two pairs of physically nonequivalent [87]Rb EFG tensors which differ in the orientation of their principal axes. In view of the presence of the twofold rotation axis parallel to the crystal a axis we expect to see two [87]Rb $1/2 \rightarrow -1/2$ transitions at $\vec{a} \perp \vec{B}_0$ and only one at $\vec{b} \perp \vec{B}_0$ and $\vec{c} \perp \vec{B}_0$. Below T_c one also expects the existence of different antiferroelectric domains. The [87]Rb EFG tensors in the 90° domains should be related by a 90° rotation around the c axis and should lead to the appearance of additional lines.

IV. [87]Rb SECOND-ORDER SHIFT OF THE $1/2 \rightarrow -1/2$ RESONANCE LINE AND LINE SHAPE IN CASE OF A RANDOM TIME-DEPENDENT PERTURBATION

The Hamiltonian of our problem is the sum of a large time-independent Zeeman term $\mathcal{H}_Z$ and a small quadrupolar term $\mathcal{H}_Q = \mathcal{H}_q^{(0)} + \mathcal{H}_Q^{(1)}(t)$ a part of which $(\mathcal{H}_Q^{(1)})$ randomly varies in time in view of the time variation of the electric-field gradient produced by the SCN$^-$ flips:

$$\mathcal{H}(t) = \mathcal{H}_Z + \mathcal{H}_Q^{(0)} + \mathcal{H}_Q^{(1)}(t) . \tag{1}$$

Here $\mathcal{H}_Q^{(1)}(t) = \mathcal{H}_Q^{(1)} f(t)$, where $f(t)$ is a function which randomly varies between $+1$ and -1. $\mathcal{H}_Q^{(0)}$ has tetragonal symmetry whereas $\mathcal{H}_Q^{(1)}$ has orthorhombic symmetry and represents the symmetry-breaking part. The ensemble average $\langle f(t) \rangle$ is zero and the correlation function $\langle f(t+t')f(t') \rangle$ is assumed to be of the form

$$\langle f(t+t')f(t') \rangle = \exp(-t'/\tau_c) . \tag{2}$$

The appropriate choice of the axis of quantization is the direction of the static applied magnetic field so that

$$\mathcal{H}_Z = -\hbar\omega_L I_z, \quad \omega_L = -\gamma(1-\sigma_{zz})B_z . \tag{3a}$$

For sake of convenience we shall for the moment neglect the time dependence of the small chemical shift contribution σ_{zz}. $\mathcal{H}_Q^{(0)}$ as well as the symmetry-breaking term $\mathcal{H}_Q^{(1)}$ can be expressed in this frame as

$$\mathcal{H}_Q^{(\alpha)} = \frac{eQ}{12} \{ V_{zz}^{(\alpha)}[3I_z^2 - I(I+1)] + V_{+1}^{(\alpha)}(I_- I_z + I_z I_-)$$
$$+ V_{-1}^{(\alpha)}(I_+ I_z + I_z I_+) + V_{+2}^{(\alpha)}I_-^2 + V_{-2}^{(\alpha)}I_+^2 \} . \tag{3b}$$

Here α is 0 or 1 and the electric-field gradient (EFG) tensor elements are $V_{\pm 1} = V_{xz} \pm iV_{yz}, V_{\pm 2} = \frac{1}{2}(V_{xx} - V_{yy}) \pm iV_{xy}$. It is useful to introduce the time-independent part of the Hamiltonian as $\mathcal{H}^{(0)} = \mathcal{H}_Z + \mathcal{H}_Q^{(0)}$. In the representation of the eigenstates of the Zeeman Hamiltonian $|-3/2\rangle$, $|-1/2\rangle$, $|1/2\rangle$, and $|3/2\rangle$ as well as in the representation of the eigenstates of $\mathcal{H}^{(0)}$ the time-dependent perturbation $\mathcal{H}_Q^{(1)}(t)$ contains both diagonal and off-diagonal elements. Such a case has been recently analyzed[8] following the work of Bjorkstam and Villa.[9] It has been shown that the time-dependent perturbation averages out in two steps as two different time scales— the Larmor frequency ω_L time scale and the much lower "site" and "90° domain" splitting time scale are involved.[8] A resonance line which is a doublet at very long correlation times τ_c in view of $\pm\mathcal{H}_Q^{(1)}$ changes into a singlet when the inverse correlation time τ_c^{-1} exceeds the doublet splitting. The $\mathcal{H}_Q^{(1)}$ induced $1/2 \rightarrow -1/2$ "orthorhombic" second-order quadrupolar shift of the resonance line vanishes, on the other hand, only when τ_c^{-1} exceeds the resonance frequencies of the main Hamiltonian, i.e., $\simeq \omega_L$. Thus three different regimes can be distinguished:

(a) In the limit of a *very short correlation time*, $\tau_c \ll \omega_L^{-1}$, the [87]Rb $1/2 \rightarrow -1/2$ transition is observed[8] at a frequency

$$\omega_{-1/2 \rightarrow 1/2} = \omega_L + \Delta\omega_{1/2 \rightarrow -1/2}^{(0)}, \quad \omega_L \tau_c \ll 1 , \tag{4a}$$

where

$$\Delta\omega_{1/2 \rightarrow -1/2} = \frac{eQ}{12\hbar^2\omega_L}(V_{-2}^{(0)}V_{+2}^{(0)} - 2V_{-1}^{(0)}V_{+1}^{(0)}) \tag{4b}$$

corresponds to the time averaged Hamiltonian $\mathcal{H}^{(0)} = \mathcal{H}_Z + \mathcal{H}_Q^{(0)}$ of tetragonal symmetry. The effects of the time-dependent symmetry-breaking perturbation are here motionally averaged out.

(b) In the limit of intermediate τ_c values

$$\omega_L^{-1} < \tau_c \ll A^{-1} \tag{5a}$$

where A is a measure of the doublet splitting

$$A = \frac{(eQ)^2}{24\hbar^2\omega_L} [V_{-2}^{(0)}V_{-2}^{(1)} + V_{+2}^{(0)}V_{+2}^{(1)}$$
$$+ 2(V_{-1}^{(0)}V_{-1}^{(1)} + V_{+1}^{(0)}V_{+1}^{(1)})] ; \tag{5b}$$

the [87]Rb $1/2 \rightarrow -1/2$ transition is observed at

$$\omega_{1/2 \rightarrow -1/2}(\tau_c) = \omega_L + \Delta\omega_{1/2 \rightarrow -1/2}^{(0)} + \Delta\omega_{1/2 \rightarrow -1/2}^{(1)}(\tau_c) . \tag{6a}$$

The additional term $\Delta\omega_{1/2 \rightarrow -1/2}^{(1)}(\tau_c)$ contains the effects of $\mathcal{H}_Q^{(1)}$:

$$\Delta\omega^{(1)}_{1/2\to-1/2}(\tau_c)=\frac{eQ}{12\hbar^2\omega_L}\left[V^{(1)}_{-2}V^{(1)}_{+2}\frac{4(\omega_L\tau_c)^2}{1+4(\omega_L\tau_c)^2}\right.$$

$$\left.-V^{(1)}_{-1}V^{(1)}_{+1}\frac{2(\omega_L\tau_c)^2}{1+(\omega_L\tau_c)^2}\right],$$

(6b)

and induces a second-order quadrupolar shift of ortho-rhombic symmetry. Here the time-dependent perturbation $\mathcal{H}^{(1)}_Q(t)$, i.e., corresponding to the symmetry of the low-temperature phase, is only partially averaged out. It affects the second-order shift of the resonance line but it does not lead to a doublet splitting, i.e., to two resolved lines corresponding to sites with EFG tensors $\underline{V}^{(0)}+\underline{V}^{(1)}$ and $\underline{V}^{(0)}-\underline{V}^{(1)}$. The doublet splitting is here still averaged out but the angular dependence of the shifts will be the one given by the perturbation $\mathcal{H}^{(1)}_Q$, i.e., it will correspond to the symmetry of the low-temperature phase.

If however τ_c becomes so short that $\omega_L\tau_c\ll 1$, expressions (6a) and (6b) become identical to expressions (4a) and (4b) and the perturbation does not affect the angular dependence of the second-order shift anymore as $\Delta\omega^{(1)}_{1/2\to-1/2}(\tau_c)\to0$.

(c) In the limit of a very long τ_c when

$$\omega_L\tau_c\gg1,\quad A\tau_c\gg1 \tag{7}$$

two $1/2\to-1/2$ resonance lines with frequencies

$$\omega_\pm=\omega_L+\Delta\omega^{(0)}_{1/2\to-1/2}+\Delta\omega^{(1)}_{1/2\to-1/2}(\tau_c=\infty)$$

$$\pm\Delta_{-1/2\to1/2}(\tau_c) \tag{8}$$

will be observed.

The doublet splitting is here determined by

$$\Delta_{-1/2\to1/2}(\tau_c)=(4A^2-1/2\tau_c^2)^{1/2}. \tag{9}$$

When $A\tau_c\gg1$ the splitting becomes $4A$ and the doublet-type resonance spectrum is the same as in case of two static low-symmetry Hamiltonians with

$$\mathcal{H}_A=\mathcal{H}_Z+\mathcal{H}^{(0)}_Q+\mathcal{H}^{(1)}_Q \tag{10a}$$

and

$$\mathcal{H}_B=\mathcal{H}_Z+\mathcal{H}^{(0)}_Q-\mathcal{H}^{(1)}_Q. \tag{10b}$$

The time-dependent perturbation $\mathcal{H}^{(1)}_Q(t)$ can be thus considered to be static when $A\tau_c\gg1$ whereas it is completely motionally averaged out when $\omega_L\tau_c\ll1$. In the intermediate region ($A\tau_c\ll1,\omega_L\tau_c\gg1$) the perturbation is only partially averaged out. The elements of the EFG tensor in the crystal fixed coordinate frame are often determined by the Volkoff method[10] from the angular dependence of the $1/2\to-1/2$ transition frequency. This method can be used in cases (a) or (c)—(i.e., for complete averaging of the time-dependent EFG tensor or for a static EFG tensor—but not in the intermediate case of incomplete averaging (b).

Of course expression (8) can be expanded in a Fourier series and the coefficients can be again determined from the angular rotation patterns. The relations between the

Fourier coefficients and the EFG tensor elements will be however different from the ones given by Volkoff.[10]

V. DETERMINATION OF ⁸⁷Rb EFG AND CHEMICAL SHIFT TENSORS IN PHASE II

Far below T_c in phase II the structure can be considered as static and the SCN⁻ group should be frozen out in an ordered configuration. Case (c) of the previous section, i.e., the limit of very long correlation times should thus apply and one can use Volkoff's method[10] to determine the static EFG tensors from the angular dependencies of the $1/2\to-1/2$ ⁸⁷Rb transition frequencies:

$$\Delta\omega_{1/2\to-1/2}(\varphi_i)=\frac{1}{\omega_L}[A_i+B_i\cos(2\varphi_i)+C_i\sin(2\varphi_i)$$

$$+D_i\cos(4\varphi_i)+E_i\sin(4\varphi_i)].$$

(11)

Here $i=a,b,c$, labels the rotation axes and the coefficients A, B, C, D, and E are known functions[10] of the EFG tensor components V_{ij}. It is possible to determine all five independent EFG tensor components from the Fourier coefficients D_i and E_i alone[11] if they are known for three mutually perpendicular rotational axes. These two Fourier coefficients are unaffected by the chemical shift tensor $\underline{\sigma}$ which enters the Zeeman part of $\mathcal{H}$ and which contributes to the $\cos(2\varphi_i)$ and $\sin(2\varphi_i)$ terms as well as to the isotropic part of the second-order shift of the $1/2\to-1/2$ ⁸⁷Rb transition. Once the EFG tensor components are known the quadrupolar contributions A_{qi}, B_{qi}, and C_{qi} to the experimental Fourier coefficients A_i, B_i, and C_i can be calculated. The differences between the experimentally observed Fourier coefficients and the ones calculated from the quadrupolar perturbation give the Fourier coefficients of the chemical shift tensor contribution:

$$A_{\sigma i}=A_i-A_{qi}=(\sigma_{jj}+\sigma_{kk})/2, \tag{12a}$$

$$B_{\sigma_i}=B_i-B_{qi}=(\sigma_{jj}-\sigma_{kk})/2, \tag{12b}$$

$$C_{\sigma i}=C_i-C_{qi}=\sigma_{jk}. \tag{12c}$$

Figure 2 shows the angular dependence of the $1/2\to-1/2$ ⁸⁷Rb transition frequency in a monodomain RbSCN single crystal at $T=360<T_c$. In agreement with the crystal symmetry considerations there are two ⁸⁷Rb central $1/2\to-1/2$ lines for $a\perp B_0$ and only one such line for $b\perp B_0$ and $c\perp B_0$. The site splitting is thus present but no domain splitting is seen. The two ⁸⁷Rb quadrupole coupling tensors $eQ\underline{V}/h$ and the two chemical shift tensor $\underline{\sigma}$ determined from the rotation patterns are

$$eQ\frac{\underline{V}}{h}=\begin{bmatrix}-0.5 & 0 & 0\\ 0 & 1.8 & \pm0.3\\ 0 & \pm0.3 & -1.3\end{bmatrix}\text{MHz},$$

$$\underline{\sigma}-\sigma_0=\begin{bmatrix}22 & 0 & 0\\ 0 & 10 & \pm13\\ 0 & \pm13 & -32\end{bmatrix}\text{ppm}.$$

(13)

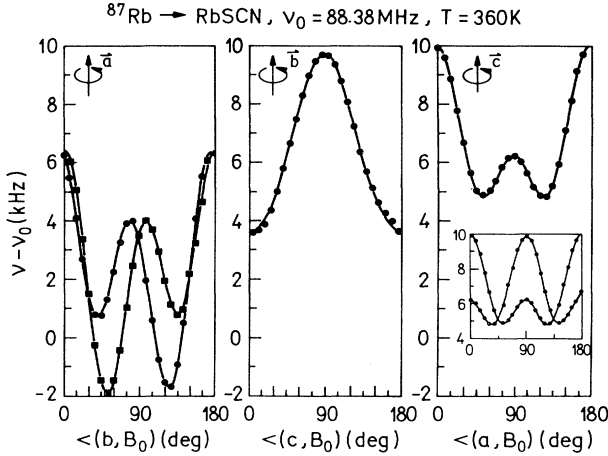^{87}Rb → RbSCN, v_0 = 88.38 MHz, T = 360 K

FIG. 2. Angular dependence of the shifts of the $1/2 \rightarrow -1/2$ ^{87}Rb NMR transitions in the antiferroelectric orthorhombic phase of RbSCN at $T = 360$ K for rotations around the crystal a, b, and c axis. The solid lines represent the fit to Eq. (11). The inset for c rotation shows the two 90° domain lines formed after the crystal was heated through T_c and cooled back in the antiferroelectric phase.

Here $\sigma_0 = \frac{1}{3}\mathrm{Tr}\underline{\sigma} = 60$ ppm is the isotropic part of the ^{87}Rb chemical shift tensor determined with respect to the ^{87}Rb resonance frequency in a RbCl solution. It should be noticed that $\underline{\sigma} - \sigma_0 = \Delta\underline{\sigma}$ is the traceless anisotropic part of the chemical shift tensor, $\mathrm{Tr}\{\Delta\underline{\sigma}\} = 0$.

In agreement with the structural data we see that the two physically nonequivalent ^{87}Rb quadrupole coupling (or EFG) tensors are chemically equivalent. Their form is compatible with the Rb sites being located on a twofold rotation axis along the a direction. This is so as one of the principal axes of the quadrupole coupling (or EFG) tensor—the one associated with $(eQ/h)V_{XX} = -0.5$ MHz—points along the crystal a axis. The other two principal axes are in the b-c plane and make an angle $\pm 6°$ with the crystal b and c directions, respectively.

The ^{87}Rb quadrupole coupling constant is

$$\frac{e^2qQ}{h} = \frac{eQV_{ZZ}}{h} = 1.84 \text{ MHz}$$

and the asymmetry parameter is

$$y = \frac{V_{XX} - V_{YY}}{V_{ZZ}} = 0.45 \ .$$

The ^{87}Rb chemical shift tensors have the same symmetry as the corresponding EFG tensors.

On heating the crystal above T_c, domains appear which remain on subsequent cooling to room temperature. These 90° domains give rise to an additional splitting of the ^{87}Rb NMR lines (inset to Fig. 2).

VI. TEMPERATURE DEPENDENCE OF THE SPECTRA

The temperature dependence of the ^{87}Rb $1/2 \rightarrow -1/2$ NMR spectra of RbSCN is shown in Fig. 3. It is obvious
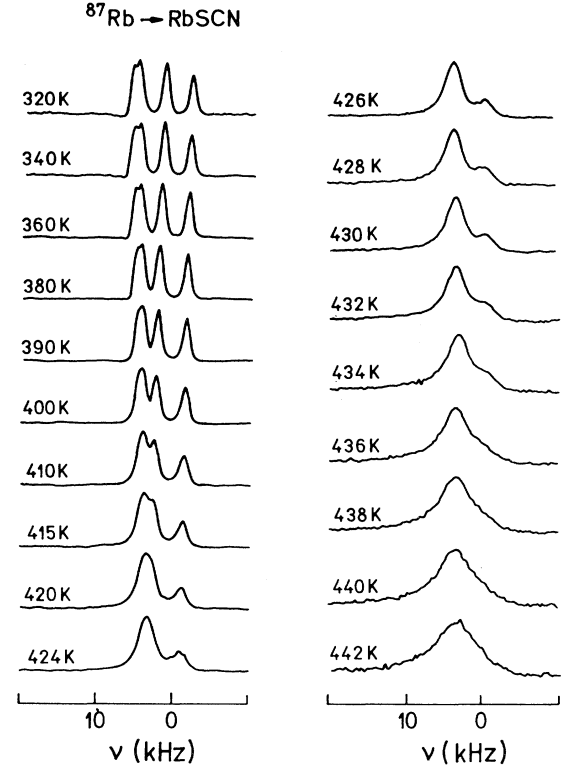
^{87}Rb → RbSCN

FIG. 3. Temperature dependence of the ^{87}Rb $1/2 \rightarrow -1/2$ NMR spectra of RbSCN at $a \perp \mathbf{B}_0, \angle(\mathbf{c}, \mathbf{B}_0) = 50°$.

that the NMR line shapes become strongly temperature dependent on approaching T_c from below. Two different effects should be mentioned:

(i) Some 40 K below T_c the lines become significantly broadened indicating the onset of incipient SCN$^-$ disorder.

(ii) The site doublet as well as the "90° domain" doublet splittings are reduced with increasing temperature. They finally vanish above T_c (Fig. 4) indicating the
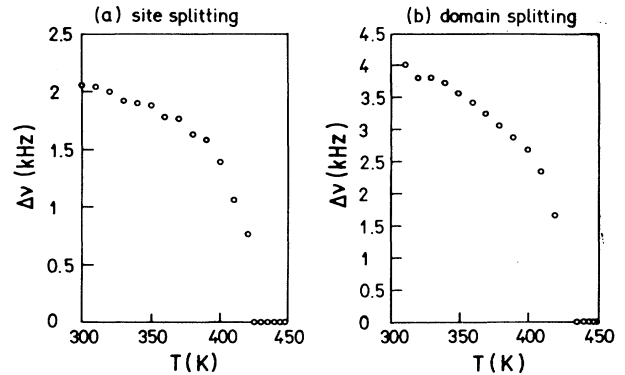

FIG. 4. (a) Temperature dependence of the splitting between the ^{87}Rb $1/2 \rightarrow -1/2$ NMR lines belonging to the two physically nonequivalent Rb sites in monodomain RbSCN $[a \perp \mathbf{B}_0, \angle(\mathbf{b}, \mathbf{B}_0) \simeq 45°]$. (b) Temperature dependence of the splitting between the ^{87}Rb $1/2 \rightarrow -1/2$ NMR lines belonging to two different 90° domains $[c \perp \mathbf{B}_0, a \| \mathbf{B}_0$, respectively, $c \perp \mathbf{B}_0, b \| \mathbf{B}_0]$.

disappearance of long-range order. The broadening of the lines close to T_c seems to be connected with the formation of microdomains[7] which are static on the neutron-scattering time scale[7] and which are embedded within a long-range ordered matrix below T_c. The microdomains of ≈ 25 Å in size are enclosed by disordered antiphase boundaries.[7] The fact that the ^{87}Rb NMR line is homogeneously broadened—as shown by two-dimensional "separation of interactions" spectroscopy[13]—demonstrates that on the NMR time scale the disorder is dynamic. The local polarization of the microdomains is fluctuating in time so that all ^{87}Rb nuclei in a given 90° macrodomain and at a given physically nonequivalent ^{87}Rb site experience the same time-averaged EFG tensor.

Let us now try to describe the temperature dependence of the ^{87}Rb NMR frequencies quantitatively. In the orthorhombic phase II there are four 90° antiferroelectric domains which are related by 0°, 90°, 180°, and 270° rotations around the crystal c axis. In these domains the Rb ions are displaced from their positions on the tetragonal fourfold axis (i.e., the 0, 0, 1/4 position) in the $\pm a$ and $\pm b$ directions. The displacement eigenvectors have the same transformation properties as the SCN$^-$ ordering eigenvectors so that these two quantities are bilinearly coupled and should thus have the same temperature dependence. Such a behavior has been indeed observed in KSCN by x-ray scattering.[4] One may ascribe for $T < T_c$ four separate ^{87}Rb EFG tensors $\underline{V}_{+a}$, $\underline{V}_{-a}$, $\underline{V}_{+b}$, $\underline{V}_{-b}$ to the four displaced Rb$^+$ sites in the a-b plane. One of the principal axes of these tensors will, due to symmetry reasons, point in the direction of the displacement, i.e., along the $\pm a$ or $\pm b$ axis. In the crystal fixed a,b,c frame these tensors will have the following forms:

$$\underline{V}_{\pm a} = \begin{bmatrix} -\alpha+\beta & 0 & 0 \\ 0 & -\alpha-\beta & \pm\gamma \\ 0 & \pm\gamma & 2\alpha \end{bmatrix} ,$$

$$\underline{V}_{\pm b} = \begin{bmatrix} -\alpha-\beta & 0 & \pm\gamma \\ 0 & -\alpha+\beta & 0 \\ \pm\gamma & 0 & 2\alpha \end{bmatrix} . \quad (14)$$

In view of the existence of long-range order the four Rb off-center sites $\pm a$ and $\pm b$ are not equivalent below T_c.

Below T_c in an $+a$ domain in which the two physically inequivalent Rb$^+$ ions are displaced along the $+a$ and $-a$ direction we can introduce the tetragonal-orthorhombic long-range order parameter as

$$S = \langle P(+a)+P(-a)-P(+b)-P(-b) \rangle , \quad (15)$$

where the P_i, $i = \pm a$, $\pm b$, describe the probabilities of occupation of the four off-center sites and the brackets $\langle \ \rangle$ stand for the ensemble average. In view of the existence of the two-fold axis along the crystal a direction we have

$$\langle P(b) \rangle = \langle P(-b) \rangle = (1-S)/4 . \quad (16)$$

As $P(a) \neq P(-a)$ we can introduce the long-range order parameter S_a which measures the ordering along the a

axis:

$$S_a = \left\langle \frac{P(+a)-P(-a)}{P(+a)+P(-a)} \right\rangle , \quad (17)$$

so that

$$\langle P(a) \rangle = (1+S)(1+S_a)/4 ,$$
$$\langle P(-a) \rangle = (1+S)(1-S_a)/4 . \quad (18)$$

If the biased motion among the four Rb sites would be fast on both NMR time scales, i.e., if both $A\tau_c \ll 1$ and $\omega_L \tau_L \ll 1$, the time-averaged EFG tensors at the two physically nonequivalent Rb sites would be for $T < T_c$:

$$\langle \underline{V} \rangle_{II \ Rb(+a)} = \frac{1+S}{2} \left[\frac{1+S_a}{2} \underline{V}_{+a} + \frac{1-S_a}{2} \underline{V}_{-a} \right] + \frac{1-S}{2} [\underline{V}_{+b} + \underline{V}_{-b}] , \quad (19a)$$

$$\langle \underline{V} \rangle_{II \ Rb(-a)} = \frac{1+S}{2} \left[\frac{1-S_a}{2} \underline{V}_{+a} + \frac{1+S_a}{2} \underline{V}_{-a} \right] + \frac{1-S}{2} [\underline{V}_{+b} + \underline{V}_{-b}] . \quad (19b)$$

For $T > T_c$, $S = S_a = 0$, $\langle \underline{V}_{Rb(+a)} \rangle = \langle \underline{V}_{Rb(-a)} \rangle$ and both EFG tensors would become axially symmetric.

If however the biased Rb ion motion is fast on the doublet splitting (≈ 3 kHz) time scale, $\tau_c A < 1$, but slow on the Larmor frequency (88 MHz) time scale, $\tau_c \omega_L > 1$, we have to use the results of Sec. IV and the second-order quadrupole shift of the $1/2 \to -1/2$ transition becomes

$$\delta = \omega_{1/2 \to -1/2} - \omega_L = f(\underline{V}^{(0)})$$
$$+ \sum_{i = +a,-a,+b,-b} \langle P(i) \rangle f(\underline{V}^{(i)}) . \quad (20a)$$

For the two $\pm a$ sites in the a domain one thus finds

$$\delta_{\pm a} = \omega^{(\pm a)}_{1/2 \to -1/2} - \omega_L$$
$$= f(\underline{V}^{(0)}) + \frac{1+S}{2} \left[\frac{1 \pm S_a}{2} f(\underline{V}^{(+a)}) + \frac{1 \mp S_a}{2} f(\underline{V}^{(-a)}) \right]$$
$$+ \frac{1-S}{4} [f(\underline{V}^{(+b)}) + f(\underline{V}^{(-b)})] . \quad (20b)$$

Similarly one obtains the second-order shift for the two $\pm b$ sites in the 90° rotated b domain:

$$\delta_{\pm b} = \omega^{(\pm b)}_{1/2 \to -1/2} - \omega_L$$
$$= f(\underline{V}^{(0)}) + \frac{1+S}{2} \left[\frac{1 \pm S_a}{2} f(\underline{V}^{(+b)}) + \frac{1 \mp S_a}{2} f(\underline{V}^{(-b)}) \right]$$
$$+ \frac{1-S}{4} [f(\underline{V}^{(-a)}) + f(\underline{V}^{(+a)})] . \quad (20c)$$

Here we used

$$f(\underline{V}^{(i)})=\frac{(eQ)^2}{12\hbar^2\omega_L}[V_{-2}^{(i)}V_{+2}^{(i)}-2V_{-1}^{(i)}V_{+1}^{(i)}] \; ;$$

$$i=\pm a, \pm b \tag{21a}$$

and

$$\underline{V}^{(i)}=\underline{V}_i-\langle\underline{V}\rangle : \tag{21b}$$

with $\underline{V}_i$ defined by Eq. (14) and

$$\langle\underline{V}\rangle=\frac{1}{4}[\underline{V}_{(+a)}+\underline{V}_{(-a)}+\underline{V}_{(+b)}+\underline{V}_{(-b)}]$$

$$=\begin{bmatrix} -\alpha & 0 & 0 \\ 0 & -\alpha & 0 \\ 0 & 0 & 2\alpha \end{bmatrix} . \tag{21c}$$

For $a\perp B_0, \angle(c,B_0)=45°$ one finds the $\pm a$ site splitting in a monodomain crystal as

$$\Delta\omega_{site}=\delta_{+a}-\delta_{-a}$$

$$=\frac{1+S}{2}S_a[f(V^{(+a)})-f(V^{(-a)})]$$

$$\propto\gamma\beta(1+S)S_a . \tag{22}$$

Close to T_c, the splitting is proportional to S_a.

The domain splitting at $c\perp B_0, a\|B_0$ or $c\perp B_0, b\|B_0$, is on the other hand, linear in S and proportional to the off-diagonal EFG tensor element γ:

$$\Delta\omega_{domain}=\delta_a-\delta_b=s[f(V^{(a)})-f(V^{(b)})]\propto\gamma^2 S . \tag{23}$$

For $c\perp B_0, a\|B_0$ $f(\underline{V}^{(+a)})=f(\underline{V}^{(-a)})$ and $f(\underline{V}^{(+b)})=f(\underline{V}^{(-b)})$ so that there is—in agreement with the experiment—no site splitting at this orientation.

From the experimental data we can thus determine the temperature dependencies of the order parameters S and S_a. The results can be compared with the prediction of the compressible pseudospin Ising model[3] which yields

$$S_a=\tanh\left[\frac{T_0}{T}S_a+A\frac{T_0}{T}S_a^3\right] . \tag{24}$$

The agreement is good if one takes $T_0=T_c=435$ K and $A=0.36$.

VII. ANGULAR DEPENDENCE
OF THE SECOND-ORDER SHIFTS ABOVE T_c

Above T_c the long-range order parameters S and S_a vanish as demonstrated in Fig. 4. This agrees with the vanishing of the intensity of the superlattice reflections in neutron scattering. According to x-ray data[4] the Rb ion
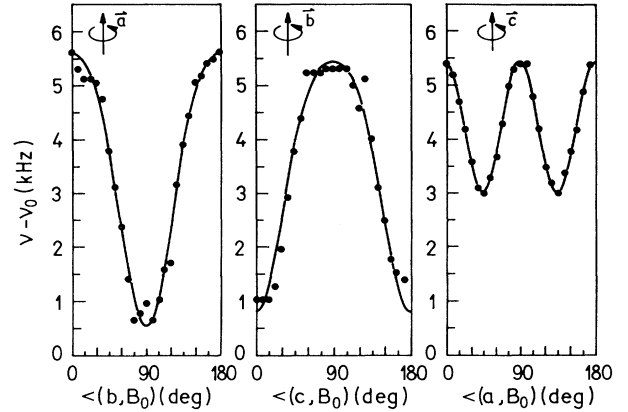

FIG. 5. Angular dependence of the shifts of the $1/2\rightarrow-1/2$ ^{87}Rb NMR transition in the high-temperature tetragonal phase of RbSCN at $T=442.5$ K for rotations around the a,b, and c axis. The solid lines represent the fit to Eq. (11).

should be located on the fourfold c axis. This would imply an axially symmetric form of the Rb EFG tensor with the longest principal axis being parallel to the c direction, $V_{ZZ}\|c$, and $V_{XX}=V_{YY}$. As it can be seen from the angular dependencies of the second-order shifts of the $1/2\rightarrow-1/2$ ^{87}Rb NMR transition (Fig. 5) this is not what is, in fact, observed.

The angular rotation pattern for the c rotation is strongly anisotropic and not isotropic as expected for $V_{ZZ}\|c, V_{XX}=V_{YY}$. This means that the symmetry of the tetragonal phase is broken on the time scale of our ^{87}Rb quadrupole perturbed NMR experiment. The same type of dynamic symmetry breaking has been observed for $T>T_c$ in KSCN by ^{39}K ($I=3/2$) NMR (Ref. 11) but not in NH$_4$ SCN by ^{14}N ($I=1$) NMR.[12]

Since the site doublet and the domain doublet splittings have already vanished, whereas the angular dependence of he second-order shift still shows orthombic rather than tetragonal symmetry, we are obviously in the case of an intermediate correlation time where partial motional averaging takes place:

$$A\tau_c\ll1, \quad \omega_L\tau_c\gg1 , \tag{25}$$

i.e., τ_c^{-1} is between 3 kHz and 88 MHz.

The motion is fast on the ^{87}Rb chemical shift tensor scale 10^{-2} s so that this tensor is effectively axially symmetric: $\sigma_{aa}=\sigma_{bb}=\sigma_\perp$.

The angular dependence of the second-order quadrupole shifts $\delta=\omega_{1/2\rightarrow-1/2}-\omega_L$ can be for $T>T_c$ quantitatively described by Eqs. (6a) and (6b) with $\omega_L\tau\gg1$ yielding

$$\delta=\frac{(eQ)^2}{12\hbar^2\omega_L}\left[(V_{-2}^{(0)}V_{+2}^{(0)}-2V_{-1}^{(0)}V_{+1}^{(0)})+\frac{1}{4}\sum_{i=+a,-a,+b,-b}(V_{-2}^{(i)}V_{+2}^{(i)}-2V_{-1}^{(i)}V_{+1}^{(i)})\right] , \tag{26}$$

where $\underline{V}^{(0)}=\langle V\rangle$ is given by (21c) and $\underline{V}^{(i)}$ by Eqs. (21b) and (14).

Physically this means that the high-temperature phase of RbSCN consists of a large number of orthorhombic microdomains or clusters with a lifetime longer than 10^{-7} s and shorter than 10^{-3} s. On this time scale the SCN molecules are *not* moving between two *equivalent* orientations separated by 180° despite the fact that long-range antiferroelectric order has disappeared. Rather they move in an asymmetric double-well single-particle potential. The two orientational states of the SCN$^-$ molecule become equivalent and the structure tetragonal only on the time average for times longer than 10^{-3} s.

The above results essentially agree with recent neutron-scattering result,[7] which show that the average size of the orthorhombic clusters is of the order of 35 Å a few degrees above T_c and decreases with increasing temperature. On the neutron-scattering time scale, 10^{-11} s, these clusters of course appear to be static.

The large moment of inertia of the SCN$^-$ dipoles and the small space available for reorientation thus result in a dramatic slowing down in the time scale of the order-parameter fluctuations. Whereas structural phase transitions are usually observed by NMR and other techniques in the fast motion limit so that one measures time-averaged observables—such as order parameters—above and below T_c, we can here study a phase transition in the slow motion limit, where time averaging is incomplete, the instantaneous structure is seen and dynamic symmetry breaking is observed above T_c. The physical picture of the structural transition that emerges is that the disordering process is connected with the formation of dynamic clusters or microdomains which are embedded in a long-range-ordered matrix below T_c and random above T_c. This agrees with the picture obtained by computer experiments.

VIII. TEMPERATURE DEPENDENCE OF THE LINEWIDTH

The same conclusions as above are also obtained from the temperature dependence of the NMR linewidth (Fig. 6). Whereas one usually finds in structural phase transi-
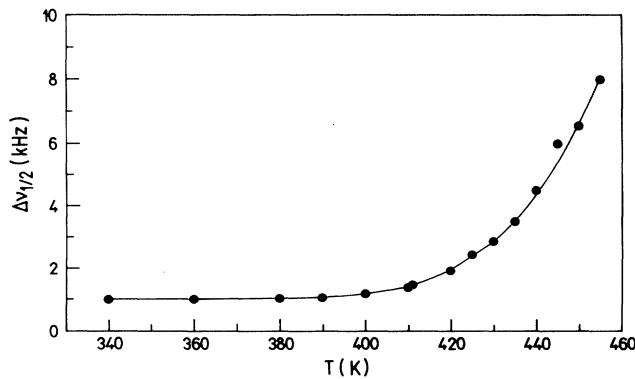
tions a peak in the NMR linewidth at T_c, in RbSCN the width of the ^{87}Rb $1/2 \rightarrow -1/2$ NMR transition continues to increase with increasing temperature on passing through T_c. No anomaly in the linewidth is seen at T_c. This demonstrates that on the time scale of our NMR linewidth experiment the same local structure is seen above and below T_c and that the thermally activated single-particle jumps in the asymmetric double-well potential for SCN$^-$ reorientations are becoming more and more frequent as the temperature increases. This is in sharp contrast to the usual "soft-mode" case where the frequency of the soft mode is always much higher than the characteristic NMR time scales and where one observes time averaged quantities above and below T_c.

IX. TEMPERATURE DEPENDENCE OF ^{87}Rb SPIN-LATTICE RELAXATION

The spin-lattice relaxation of the ^{87}Rb central $1/2 \rightarrow -1/2$ transition is generally two exponential with the relaxation rates $2W_1$ and $2W_2$.[14] Here W_1 and W_2 represent the lattice-induced transition probabilities per unit time for the $\pm 3/2 - \pm 1/2$ transitions and for the $\pm 3/2 - \mp 1/2$ transitions, respectively.

The temperature dependence of the two spin-lattice relaxation times $T_{1a}=(2W_1)^{-1}$ and $T_{1b}=(2W_2)^{-1}$ is for two Larmor frequencies: 124.4 and 88.3 MHz shown in Fig. 7. Within the experimental resolution the four spin-lattice relaxation times continuously decrease with increasing temperature and pass the phase transition with nearly no change in either the values or the slopes at T_c. The spin-lattice relaxation rates at 88.3 MHz are by ap-

FIG. 6. Temperature dependence of the width of the ^{87}Rb NMR $1/2 \rightarrow -1/2$ line in RbSCN in the vicinity of T_c. The solid line is a guide to the eye.
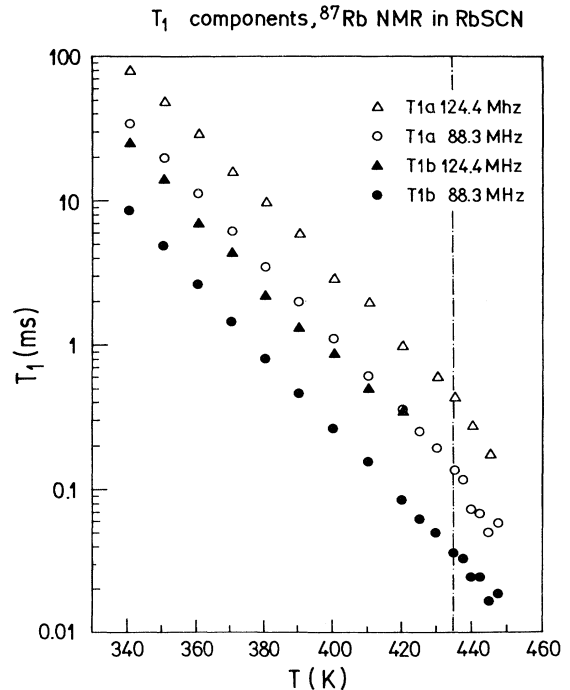

FIG. 7. Temperature dependence of the ^{87}Rb spin-lattice relaxation times in RbSCN at the Larmor frequencies of 124.4 and 83.3 MHz.

proximately a factor of 2 shorter than the spin-lattice relaxation times at 124.4 MHz.

The motion which dominates the rubidium spin-lattice relaxation is thus within the experimental resolution not affected by the phase transition. The ratio of the relaxation times at 124.4 and 88.3 MHz which is within the experimental resolution equal to $(124.4 \text{ MHz}/88.3 \text{ MHz})^2$ shows that this motion is slow as compared to the Larmor precession (10^8 Hz). This motion which may be—as proposed earlier—the reorientation of the SCN groups in an asymmetric double-potential well is, on the other hand, faster than the reorientation of microdomains at least by an order of magnitude. In such a case namely the reorientation of the microdomains influences T_1 for less than 10%. Thus the characteristic time of the reorientation of the microdomains must be longer than 10^{-7} s in agreement with the linewidth data.

X. CONCLUSION

The ^{87}Rb NMR data confirm the existence of microdomains of the low-temperature phase in the high-temperature phase of RbSCN. Within each domain there is a motion which dominates the ^{87}Rb NMR linewidth and spin-lattice relaxation. We propose this motion to be the reorientation of the SCN groups in an asymmetric double-potential well. The characteristic time of the reorientation of the SCN dipoles is above and below T_c longer than 10^{-8} s. The characteristic time of the reorientation of the microdomains is at least by an order of magnitude longer, i.e., longer than 10^{-7} s. On the other hand, the quadrupole perturbed NMR frequencies in the high-temperature phase show that the characteristic time of the reorientation of microdomains in the high-temperature phase is shorter than 10^{-3} s.

[1]W. Klement and C. Pistorius, Bull. Chem. Soc. Jpn. **49**, 2148 (1976).

[2]Y. Yamada and T. Watanabe, Bull. Chem. Soc. Jpn. **36**, 1032 (1963); C. Akers, S. W. Peterson, and R. D. Willet, Acta Crystallogr. B **24**, 1125 (1968).

[3]W. Schranz, H. Warhanek, R. Blinc, and B. Žekš, Phys. Rev. B **40**, 7141 (1989).

[4]S. Yamamoto, M. Sakuno, and Y. Shinnaka, J. Phys. Soc. Jpn. **56**, 4393 (1987).

[5]V. Janovec, W. Schranz, H. Warhanek, and Z. Zigmund, Ferroelectrics **98**, 171 (1989).

[6]W. Schranz, H. Warhanek, and P. Zielinski, J. Phys. C **1**, 1141 (1989).

[7]O. Blaschko, W. Schranz, and A. Fuith, J. Phys. Condens. Matter **6**, 1 (1994).

[8]J. Seliger, J. Magn. Reson. A **103**, 175 (1993).

[9]J. L. Bjorkstam and M. Villa, Phys. Rev. B **22**, 5025 (1980).

[10]G. M. Volkoff, Can. J. Phys. **31**, 820 (1953).

[11]R. Blinc, J. Seliger, T. Apih, J. Dolinšek, I. Zupančič, O. Plyusch, A. Fuith, W. Schranz, H. Warhanek, B. Topič, and U. Haeberlen, Phys. Rev. B **43**, 569 (1991).

[12]R. Blinc, J. Selinger, V. Žagar, T. Apih, J. Dolinšek, H. Warhanek, A. Fuith, and W. Schranz, Phys. Rev. B **42**, 8125 (1990).

[13]J. Dolinšek, J. Magn. Reson. **92**, 312 (1991).

[14]J. Selinger and R. Blinc, J. Phys. Condens. Matter **5**, 9401 (1993).